

## Research Article

# Synthesis and Characterization of *Grewia asiatica*-Stabilized Silver Nanoparticle as a Selective Probe for Al<sup>3+</sup> in Tap, Deionized, Industrial Waste Water and Human Blood Plasma

Nasreen Begum <sup>1,2</sup>, Itrat Anis,<sup>1</sup> Shazia Haider,<sup>3</sup> Tabinda Zarreen Mallick,<sup>4</sup> and Muhammad Iqbal Chaudhary<sup>2</sup>

<sup>1</sup>Department of Chemistry, University of Karachi, Karachi 75270, Pakistan

<sup>2</sup>H. E. J. Research Institute of Chemistry, International Center for Chemical and Biological Sciences, University of Karachi, Karachi 75270, Pakistan

<sup>3</sup>Department of Pharmaceutical Chemistry, Faculty of Pharmacy and Pharmaceutical Sciences, University of Karachi, Karachi 75270, Pakistan

<sup>4</sup>Department of Pharmaceutical Chemistry, Jinnah Sindh Medical University, Karachi, Pakistan

Correspondence should be addressed to Nasreen Begum; [alinasreen29@yahoo.com](mailto:alinasreen29@yahoo.com)

Received 7 November 2023; Revised 2 May 2024; Accepted 21 May 2024; Published 29 May 2024

Academic Editor: Cristina Femoni

Copyright © 2024 Nasreen Begum et al. This is an open access article distributed under the Creative Commons Attribution License, which permits unrestricted use, distribution, and reproduction in any medium, provided the original work is properly cited.

Aluminum can be found in water and vegetables in the form of the trivalent ion (Al<sup>3+</sup>), which can potentially contaminate food and water. Overconsumption of aluminum can lead to serious health problems in humans. Therefore, there is a need for an economical and simple procedure to detect the presence of aluminum. In this study, we synthesized a conjugate of *Grewia asiatica* extract with silver nanoparticles. The nanoparticle-stabilized fruit extract of *Grewia asiatica* was found to be an extremely selective sensor of Al<sup>3+</sup> in tap water, DI water, industrial wastewater, and human blood plasma. We characterized the *Grewia asiatica*-conjugated silver nanoparticles (GA-AgNPs) using UV-visible, SEM, and AFM techniques and found that they were stable in an extensive pH range and different electrolyte concentrations up to 10 M NaCl. The GA-AgNPs were circular in shape with typical particle sizes of 65–97 nm. We inspected the photo physical properties of GA-AgNPs concerning metallic ions using UV-visible spectroscopy and found that they were highly selective for Al<sup>3+</sup> ions, with no interfering ions detected in competitive experimentation. The absorption intensity of GA-AgNPs was directly related to Al<sup>3+</sup> concentration over a wide range of concentrations (6.25–500 μM). Jobs plot experiment displayed 1:1 binding stoichiometry between GA-AgNPs, and Al<sup>3+</sup>. Additionally, GA-AgNPs were effectively utilized for the recognition of Al<sup>3+</sup> in laboratory tap water, DI water, industrial wastewater, and human blood plasma.

## 1. Introduction

Aluminum is the third most abundant metal in the earth's crust and is widely used in various industries. Trivalent ion (Al<sup>3+</sup>) is found in water and vegetables, which can enter the human body through food and water sources [1]. The World Health Organization (WHO) states that the average daily exposure of humans to Al (III) is about 3 to 10 mg·kg<sup>-1</sup>. However, the extensive use of aluminum in daily life, such as in the form of aluminum foil, cookware, containers,

pharmaceuticals, and food additives [2], can lead to contamination of food and water with Al<sup>3+</sup> and pose health risks. Even a small amount of Al<sup>3+</sup> can cause various health problems, according to several epidemiological studies. Overconsumption of aluminum can cause idiopathic Parkinson's disease [3], memory impairment, impairment to the central nervous system, dialysis encephalopathy, and Alzheimer's disease [4]. The concentration of Al<sup>3+</sup> ions in the brain should not exceed 2 mg/g of brain tissue, and the World Health Organization (WHO) and the Environmental

Protection Agency (EPA) have set the allowable limit of Al (III) in drinking water as  $7.4\ \mu\text{M}$  or 50 ppm, respectively. Therefore, it is important to develop detection methods that can identify trace levels of Al (III) for economic and health reasons [5–7]. Several methods are currently used for Al (III) detection, such as atomic absorption spectrometry (AAS) [8], graphite furnace- atomic absorption spectrometry (GF-AAS), inductively coupled plasma mass spectrometry (ICP-MS), inductively coupled plasma atomic emission spectrometry (ICPAE-MS), and electrochemical methods, etc. However, these methods have limitations such as complex sample preparation, high background signals [7], and expensive instrumentation. Therefore, more efficient and accurate methods are needed for the detection of Al (III).

It is imperative to have a feasible, inexpensive, quick, and eco-friendly method for recognizing Al (III). Nanoparticles of noble metals possess optical, chemical, electrochemical, and mechanical properties that make them ideal for various applications such as biocatalysis cosmetics, coating, and anticancer [9]. Recent developments such as paper-based analytical devices (PAD), colorimetric assays, quantum-dots-based photoelectrochemical immune assays, magnetic bead-centered reverse colorimetric sensors,  $\text{MnO}_2$  nano-flakes with enzyme torrent intensification for colorimetric immunoassay, and Fenton reaction-centered colorimetric immunoassay have enabled colorimetric recognition in aqueous systems for metal ions [10–22]. The accumulation of NPs induced by the target analyte is central to a graphic color alteration. Similarly, changes in their associated absorption spectra help in the detection of analytes without the need for complex instruments. Metal nanoparticles serve as sensing probes, due to their narrow size distribution, functionalized surface, high aspect ratio, and distinctive band of SPR [23–25]. Specific NPs like silver, copper, and gold, having trivial size and distinctive confined SPR, are used for the improvement of ocular devices. Due to their exceptional SPR and physicochemical properties, they have been widely used for target analyte detection at the trace level [26–29]. AgNPs are more appropriate than AuNPs for recognition since they have a 100-fold better molar extinction coefficient, giving them a greater contemplation in absorption spectroscopy [30]. In this study, we have established an eco-friendly recognition technique for Al (III) with a lower limit of detection of  $0.0412\ \mu\text{M}$  via UV spectrophotometer. The limit of detection of the current method is  $0.04129\ \mu\text{M}$ , and the method is green synthesis. However, previously,  $0.0405\ \mu\text{M}$  LOD was recorded by using citrate and polyvinyl pyrrolidone through the chemical reduction method as mentioned in Table 1. We have used AgNPs conjugated with the fruit extract of *G. asiatica* (GA-AgNPs) for the highly sensitive and discriminating recognition of  $\text{Al}^{3+}$  in aqueous medium. The research also focused on detecting  $\text{Al}^{3+}$  via an optical color alteration as compared to other globally important metallic ions.  $\text{Al}^{3+}$  ion was detected in water samples within 30–35 seconds. The recognition profile of GA-AgNPs was discovered through UV-visible spectroscopy. A considerable decrease in the absorption strength of GA-AgNPs was noticed upon adding  $\text{Al}^{3+}$ , while all other tested metals did

not produce any substantial change in the SPR band. Moreover, GA-AgNPs-based sensors effectively detected  $\text{Al}^{3+}$  in tap, deionized, and industrial waste water, as well as in human blood plasma.

## 2. Experimental Section

**2.1. Materials and Methods.** All the reagents were procured from viable dealers and consumed deprived of additional purifications. Glassware was washed with DI water before use. Solo-step synthesis of NPs was conceded via the reduction of  $\text{Ag}^{+1}$  to Ag atoms consuming *G. asiatica* fruit extract. The absorption spectra indicate the creation of GA-AgNPs (Figure 1). The UV-visible spectra were detailed on a spectrophotometer with a 1.0 cm path length (Thermo Scientific Evolution 300, USA). The pH was detailed on a numeral pH meter of model-510 (Oakton, Eutech, Singapore), fitted out using a functioning electrode of glass, whereas Ag/AgCl was utilized as a reference electrode. AFM analysis was completed via Agilent 5500, run in the tapping mode (Germany). SEM investigation was supported on the JSM-6380A appliance with a tester coater (JFC-1500) (Jeol Japan).

**2.2. Grounding of *Grewia asiatica* Extract.** 400g of *Grewia asiatica* fruit was purchased from a local marketplace and carefully washed. The seeds were separated from the fruit, and the pulp was dried at room temperature in the shade. The dried pieces were ground and soaked in 95% ethanol (1 : 4) followed by the addition of 5 mL of 0.1% HCl. The mixture was left for 72 hours. The resulting extract was filtered using Whatman No. 1 filter paper, and the solvent was evaporated at reduced pressure to obtain 130.718 g of extract. The extract was then refrigerated until further use.

**2.3. Synthesis of GA-AgNPs.** GA-conjugated AgNPs were produced using a green synthesis method. Fruit extract was used as a reducing and stabilizing agent. The process involved heating 100 mL of  $\text{AgNO}_3$  (0.5 mM) to 40–50°C and slowly adding 10 mL of GA (0.1256 g/100 mL  $\text{H}_2\text{O}$ ) fruit extract. The maximum absorption by GA-AgNPs occurred at a ratio of (10 : 1) (Ag : GA v/v). The reaction mixture was stirred for about 20 minutes resulting in a yellowish-brown mixture. The mixture was stirred for an additional 2–3 hours. The resulting GA-AgNPs were then centrifuged at a rate of 10,000 rpm for 12 minutes, and UV spectra were used to validate the nanoparticles. The solution was diluted up to 6 times with DI- $\text{H}_2\text{O}$  to obtain a firm SPR.

**2.4. Preparation of Different Metal Salt Solutions.** 500  $\mu\text{M}$  solutions of different metals including  $\text{Na}^{1+}$ ,  $\text{K}^{1+}$ ,  $\text{NH}^{1+}$ ,  $\text{Ca}^{2+}$ ,  $\text{Ba}^{2+}$ ,  $\text{Mg}^{2+}$ ,  $\text{Pb}^{2+}$ ,  $\text{Ni}^{2+}$ ,  $\text{Co}^{2+}$ ,  $\text{Sn}^{2+}$ ,  $\text{Cu}^{2+}$ ,  $\text{Zn}^{2+}$ ,  $\text{Pb}^{2+}$ ,  $\text{Bi}^{3+}$ , and  $\text{Al}^{3+}$  were prepared by dissolving the calculating amount of these salts and make up with water. Then, 2 mL of these salt solutions was mixed with 2 mL of GA-AgNPs, and UV-vis spectra were recorded.

TABLE 1: Different methods for the detection of  $\text{Al}^{3+}$ .

Method	Functionalizing agent	Limit of detection	Detection tool	Comment	Reference
Calorimetric	Schiff base	$0.29 \mu\text{M}$	Pentapeptide (CALNN)	Chemical reduction	[31]
Calorimetric	Pyridoxyl derivative	$0.51 \mu\text{M}$	AuNPs	Complex procedure	[32]
Calorimetric	Schiff base	$0.29 \mu\text{M}$	AuNPs	Complex procedure	[33]
Calorimetric	Polyacrylate	$2.0 \mu\text{M}$	PAA-AuNPs	Sun light induced synthesis	[9]
Fluorescence	Nitrogen-doped carbon dots (N-CDs)	$0.0097 \mu\text{M}$	Carbon dots	Complex procedure	[34]
Calorimetric	Aluminon	0.001 ppm	AgNPs	Chemical reduction	[35]
Calorimetric	Citrate and polyvinyl pyrrolidone	$0.0405 \mu\text{M}$	AgNPs	Chemical reduction	[36]
UV-visible	<i>Grewia asiatica</i> L. (fruit)	$0.0413 \mu\text{M}$	AgNPs	Green synthesis	Current work

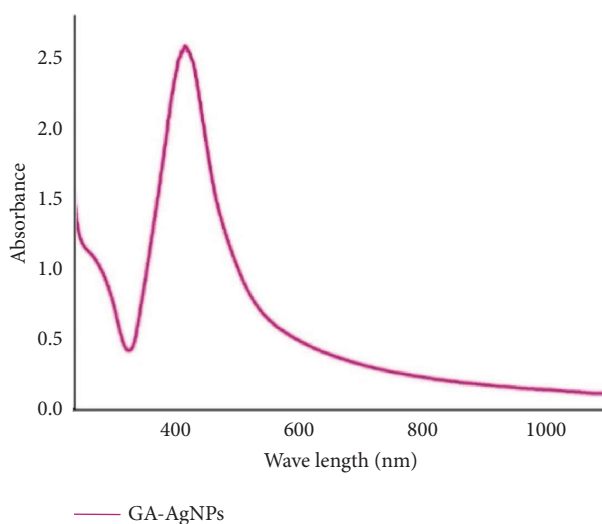


FIGURE 1: UV-visible spectrum showing GA-AgNPs.

**2.5. Spiking in Tap, Deionized, and Industrial Waste Water.** Water samples were collected from three different sources: tap water, deionized water from HEJRIC, and industrial waste water from Sonic Textile Industries Private Limited. The industrial waste water was spiked with a known concentration of  $\text{Al}^{3+}$ . A solution of 2 mL of GA-AgNPs was mixed with 2 mL of each water sample containing  $\text{Al}^{3+}$ , and the UV spectra were recorded.

**2.6. Spiking in Blood Plasma.** Blood plasma was extracted from volunteers through a pinhole after obtaining approval from the ethics committee of the institute. The human blood was centrifuged at 4,000 rpm for approximately 6 minutes to separate the plasma at  $25^\circ\text{C}$ . Two solutions were prepared. One solution was kept as a blank, while the other was spiked with  $100 \mu\text{L}$  of GA-AgNPs [37].

### 3. Results and Discussion

**3.1. Synthesis Mechanism of GA-AgNPs.** GA-AgNPs were produced using sustainable synthetic methods. The formation of GA-AgNPs was indicated by the presence of a distinctive SPR peak at 414 nm in the obscure brown mixture resulting from the bio reduction of GA-AgNPs (Figure 1). The maximum absorption by GA-AgNPs

occurred at a ratio of (10:1) (Ag:GA v/v). A series of studies were conducted to determine the optimal mole ratio between the ligand and the metallic ion.

**3.2. Size Dissemination of GA-AgNPs.** The size and shape of GA-AgNPs were determined using SEM and AFM techniques. It was observed that the nanoparticles were distributed in varying sizes. The size of the NPs ranged from 65 to 97 nm. Smaller sized NPs formed aggregates that appeared as large particles (Figures 2(a) and 2(b)). SEM analysis showed that the nanoparticles had a slightly spherical shape, as depicted in Figure 2(c). The produced AgNPs remained unchanged and stable for approximately 240 days.

**3.3. Stability of GA-AgNPs.** It is important for nanoparticles to remain stable for practical applications. Factors such as changes in pH, electrolyte concentration, and temperature can affect the stability of these particles. The stability of GA-AgNPs was studied under various physiological factors. Generally, the destabilization of nanoparticles occurs by adding electrolytes. To investigate this, different concentrations of NaCl solution were added to GA-AgNPs, and their UV spectra were recorded, as shown in Figure 3. It was found that GA-AgNPs remained highly stable even after

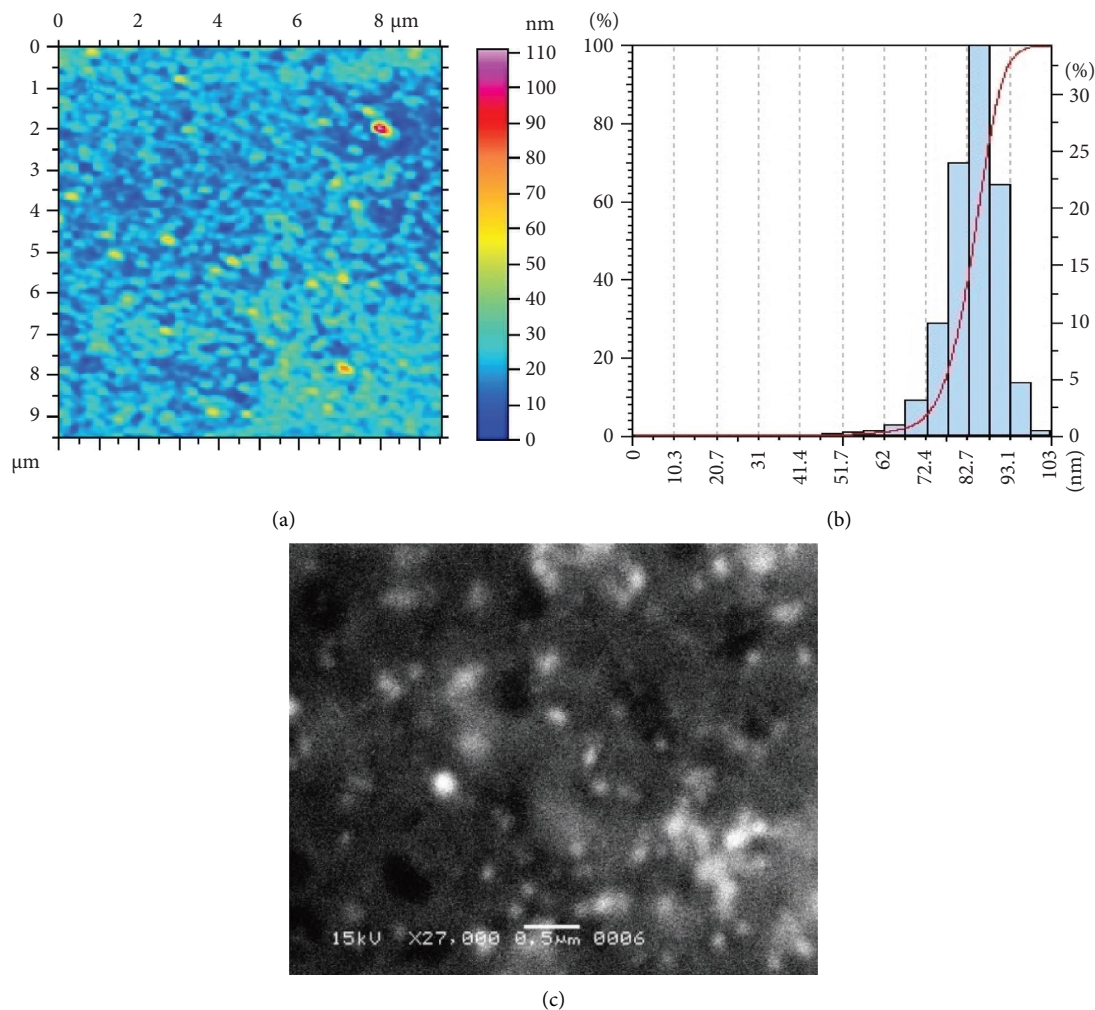


FIGURE 2: (a) AFM phantasmagorias of GA-AgNPs, (b) histogram presentation size dissemination of GA-AgNPs, and (c) SEM imaginings of GA-AgNPs.

adding 10 M of NaCl, as there was no significant change observed in the absorption intensity of GA-AgNPs. The impact of pH on the stability of NPs was also assessed, as revealed in Figure 4. The pH of GA-AgNPs was adjusted by adding dilute NaOH and HCl solutions. The nanoparticles were found to be highly stable between pH 3-10. To assess the effect of temperature, NPs were boiled at 100°C for about half an hour, and their absorption spectra were recorded. The results showed that GA-AgNPs remained constant even at 100°C, as presented in Figure 5.

**3.4. GA-AgNPs as a Sensing Probe for  $Al^{3+}$ .** The ability of GA-AgNPs to detect metal ions was evaluated using UV-vis spectroscopy. Fifteen different metal salts comprising alkali alkaline earth metals, and transition were selected, and the changes in the SPR bands of GA-AgNPs were analyzed after the addition of metal salts. The metal salt solutions (500 μM) used in this study included  $Na^+$ ,  $K^+$ ,  $NH^+$ ,  $Ca^{2+}$ ,  $Ba^{2+}$ ,  $Mg^{2+}$ ,  $Pb^{2+}$ ,  $Ni^{2+}$ ,  $Co^{2+}$ ,  $Sn^{2+}$ ,  $Cu^{2+}$ ,  $Zn^{2+}$ ,  $Pb^{2+}$ ,  $Bi^{3+}$ , and  $Al^{3+}$ . The UV-vis spectra of GA-AgNPs remained unchanged after the addition of most metal ions except for  $Al^{3+}$ . Interestingly,

significant quenching was observed when  $Al^{3+}$  was added, along with minor red shifts in the absorption intensities of GA-AgNPs, as shown in Figure 6. The other metal ions tested did not result in any noteworthy changes in the absorption strength of GA-AgNPs. These results suggest that GA-AgNPs has a specific binding site for the  $Al^{3+}$  ion (Figure 13).

**3.5. Effect of Concentration.** Conducting a concentration study is essential to determine the limit of detection (LOD) of GA-AgNPs, which is a critical feature of any sensor system including nanosensors. In this study, various concentrations of  $Al^{3+}$  ranging from 6.25 μM to 500 μM were added to a constant concentration of GA-AgNPs. UV-vis spectra were then recorded to observe the change in the Surface Plasmon band of GA-AgNPs. As shown in Figure 7, the increase in the concentration of  $Al^{3+}$  resulted in a decrease in the intensity of GA-AgNPs while simultaneously causing a red shift. The change in the absorption intensity of GA-AgNPs was found to be directly proportional to the concentration of  $Al^{3+}$  across a wide range of concentrations

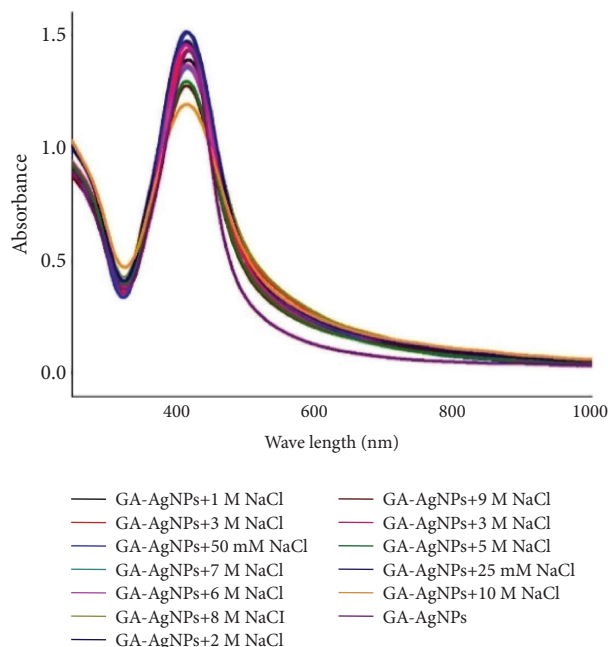


FIGURE 3: Influence of electrolyte concentrations on the strength of GA-AgNPs.

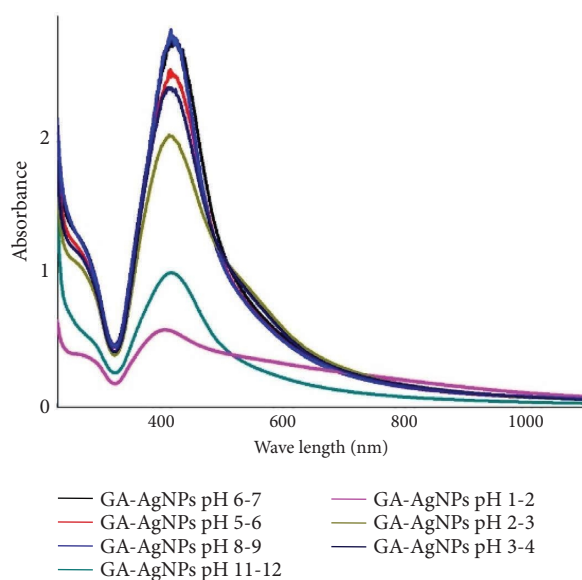


FIGURE 4: Effect of pH on the stability of GA-AgNPs.

(6.25–500  $\mu\text{M}$ ). To calculate the limits of detection quantification, we used the formula:  $\text{LOD} = 3.3 \times \text{SD}/\text{Slope}$  and  $\text{LOQ} = 10 \times \text{SD}/\text{Slope}$ . The LOD was found to be 0.0413  $\mu\text{M}$ , while the LOQ was determined to be 0.1251  $\mu\text{M}$ .

**3.6. Influence of pH on Complex Formation of GA-AgNPs and  $\text{Al}^{3+}$ .** The construction and distortion of the bond between metal ions and ligands depend on the pH of the medium. Figure 8 illustrates the effect of changes in pH on the bond formation between GA-AgNPs and  $\text{Al}^{3+}$ . Equal amounts of GA-AgNPs and aluminum were mixed, and the pH of the

solution was adjusted to a wide range of 2–12 by adding dilute solutions of HCl and NaOH. The absorption intensity of GA-AgNPs was measured across the pH range of 2–14, and significant changes in the UV-Vis spectra were observed.

**3.7. Interference Study.** The key feature of a successful sensor system depends on the ability to selectively detect a specific analyte in the presence of other similar analytes. In order to ensure the selectivity of GA-AgNPs for aluminum, sustainable tests were conducted. Equal

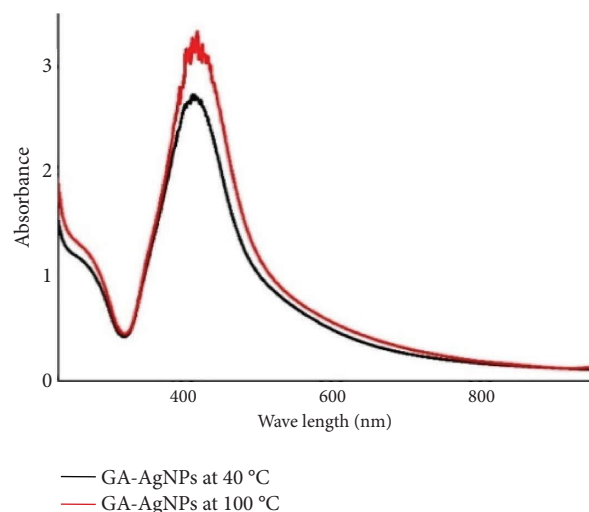


FIGURE 5: Effect of temperature changes on the stability of GA-AgNPs.

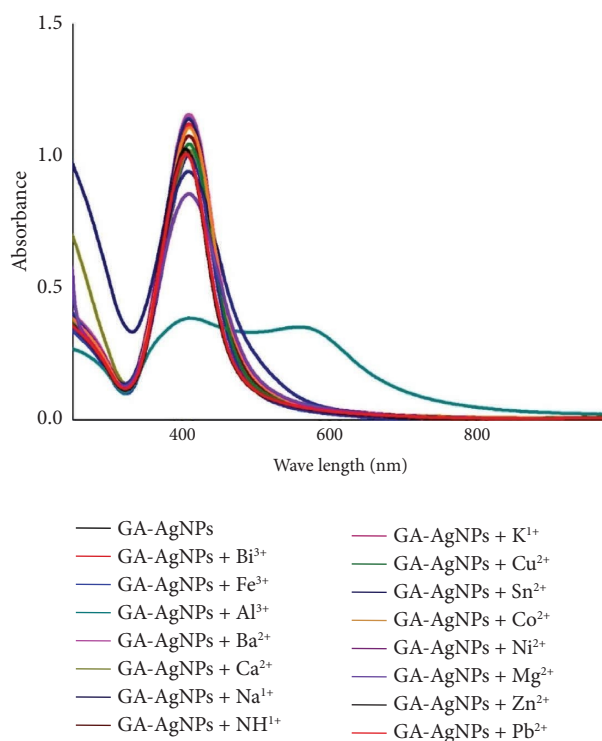


FIGURE 6: Alteration in absorption intensities of GA-AgNPs upon adding diverse metal ions.

amounts of aluminum and GA-AgNPs were mixed, and various interfering metal salt solutions ( $500 \mu\text{M}$ ) were added to this mixture. UV-vis spectra were then obtained and analyzed. As shown in Figure 9, a significant reduction in intensity, along with a slight shift towards the red end of the spectrum, was observed in the absorption spectrum of GA-AgNPs upon the addition of several metal ions. These results indicate that other metal ions do not affect the detection of  $\text{Al}^{3+}$ . Therefore, GA-AgNPs are selective for  $\text{Al}^{3+}$  even in the presence of various other metal salt ions.

**3.8. Jobs Plot.** The Jobs plot system was used to determine the binding stoichiometry between GA-AgNPs and aluminum. During the experiment, mole fractions of both GA-AgNPs and  $\text{Al}^{3+}$  were altered between 0 and 0.9 while maintaining the same volume. The two solutions were mixed in varying mole fractions, and absorption spectra were recorded. The change in absorption strength of GA-AgNPs was observed as a function of  $\text{Al}^{3+}$  mole fractions (as shown in Figure 10). The results indicated a 1 : 1 (GA-AgNPs :  $\text{Al}^{3+}$ ) binding stoichiometry between GA-AgNPs and aluminum, with extreme quenching detected at a mole fraction of 1.5.



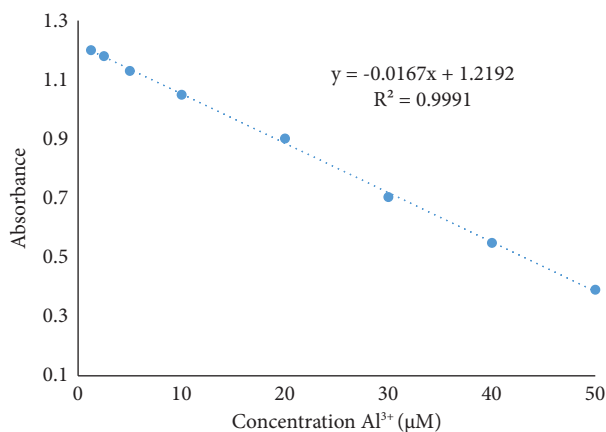


FIGURE 7: Variation in absorption intensities of GA-AgNPs upon adding diverse concentrations of Al<sup>3+</sup> (straight line equation).

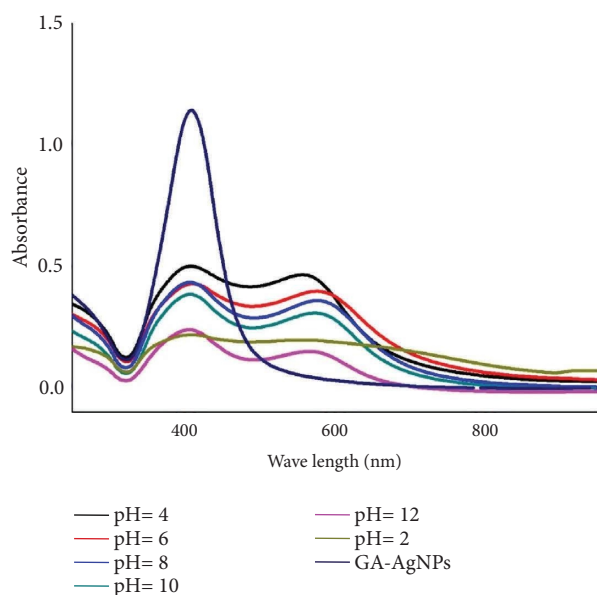


FIGURE 8: Effect of pH on the complex formation between GA-AgNPs, and Al<sup>3+</sup>.

**3.9. Analytical Applications.** Trials were conducted to investigate the impact of organic and ecological matrix on the recognition of Al<sup>3+</sup>. Laboratory tap, deionized, industrial waste water, and hominoid blood plasma samples were tested. Tap water was collected from the HEJRIC laboratory and spiked with a known concentration of Al<sup>3+</sup> (500 μM). Aluminum solutions were prepared in tap, deionized, and industrial waste waters, mixed with GA-AgNPs, and their absorption spectra were recorded under comparable conditions, as shown in Figure 11. Almost similar quenching in the pattern of absorption intensity along with a red shift was observed in tap, deionized, and industrial waste water samples, indicating that other elements of water samples do not impede the recognition of Al<sup>3+</sup>. Furthermore, hominoid blood plasma samples were spiked with a known concentration of Al<sup>3+</sup>, and changes in the absorption spectra were

recorded, as presented in Figures 12 and 13. This study revealed that the components of water and blood plasma samples do not appear to affect the recognition of Al<sup>3+</sup>. Therefore, GA-AgNPs have potential applications for the recognition of Al<sup>3+</sup> in ecological and organic samples.

**3.10. Comparison with Other Study.** The supplementary methods used for discriminating recognition of Al<sup>3+</sup> in biological and water tasters had several limitations, as presented in Table 1. Therefore, a model spectrophotometric process was developed with exceptional sensitivity and discrimination to selectively detect aluminum in the presence of other cations. This approach is an alternative to other exclusive and time-consuming instrumental techniques for the recognition of aluminum, as shown in Table 1.

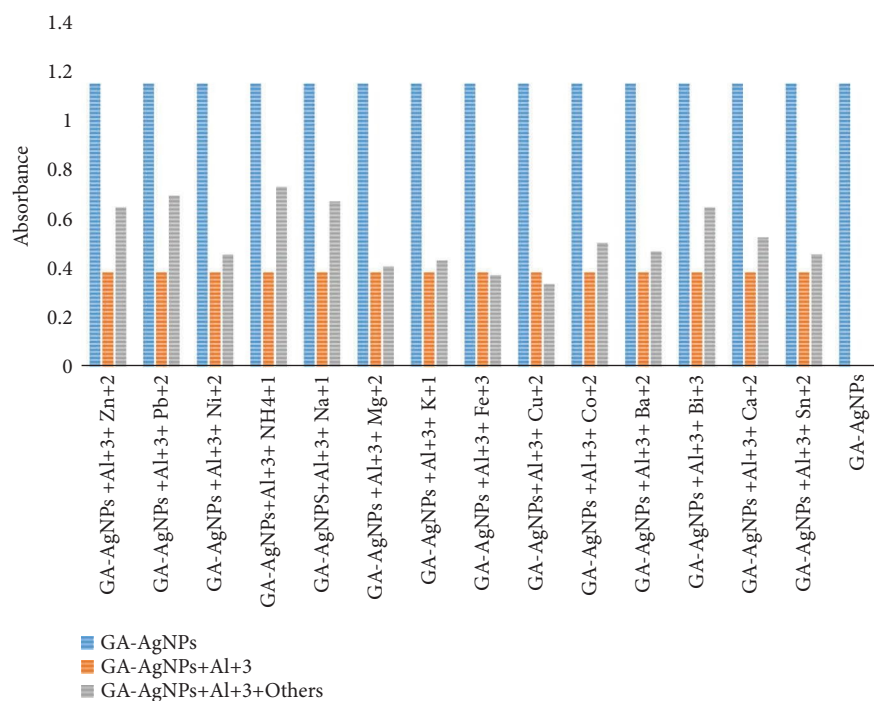


FIGURE 9: Effect of interfering metals ions on the recognition of Al<sup>3+</sup> by GA-AgNPs (3 replicates).

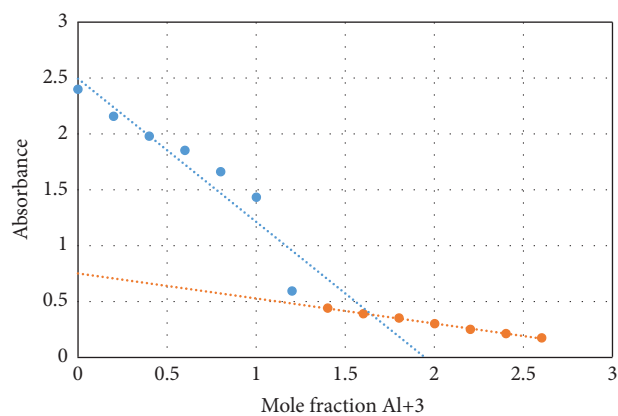


FIGURE 10: Jobs plot for finding of binding stoichiometry between GA-AgNPs, and Al<sup>3+</sup>.



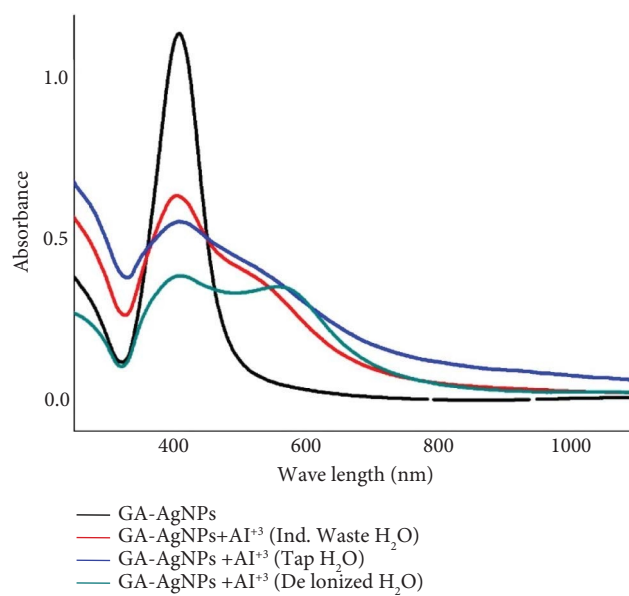
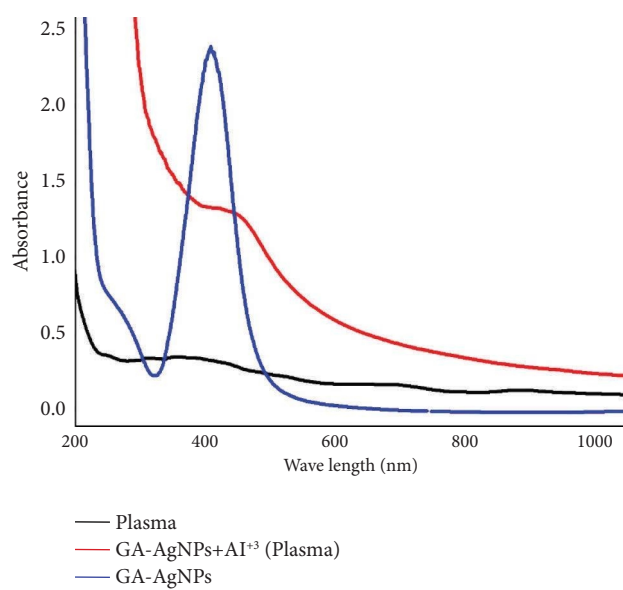
FIGURE 11: Detection of Al<sup>3+</sup> in laboratory tap, deionized, and industrial waste water.FIGURE 12: Detection of Al<sup>3+</sup> in human blood plasma samples.

FIGURE 13: GA-AgNPs and GA-AgNPs + aluminum.

#### 4. Conclusion

We have developed a new type of chemosensor using silver nanoparticles made from the extract of *Grewia asiatica* fruit (GA-AgNPs). This sensor is designed to detect  $\text{Al}^{3+}$  in a range of different samples including tap water, deionized water, industrial waste water, and human blood plasma. The GA-AgNPs were created using a green synthetic method and characterized using UV-visible, AFM, and SEM techniques. The nanoparticles were found to be circular in shape with a typical size ranging from 65 to 97 nm. The detection properties of GA-AgNPs were tested using UV-vis spectroscopy, and it was determined that adding  $\text{Al}^{3+}$  resulted in significant quenching and a red shift in the absorption intensity of the nanoparticles. GA-AgNPs were found to be highly selective for  $\text{Al}^{3+}$  and did not detect any interference from other metal ions across a wide range of pH levels. Additionally, GA-AgNPs were effectively used to detect  $\text{Al}^{3+}$  in various samples including laboratory tap water, deionized water, industrial waste water, and human blood plasma. The limit of detection of the current method is  $0.04129 \mu\text{M}$  by the green method, while previously, it was reported through the chemical reduction method. This is novelty of the current work.

#### Data Availability

The data used to support the findings of this study are included in the article.

#### Conflicts of Interest

The authors declare that they have no conflicts of interest.

#### Authors' Contributions

The corresponding author has contributed in origin and design or investigation and elucidation of the data. All authors have contributed in conscripting the article and reviewing it disparagingly for important intellectual content and consent of the final version.

#### References

- [1] J. Malini and M. Sayed, "1'-hydroxy-2'-acetonaphthone: a simple fluorescence turn-on signaling probe with high selectivity and sensitivity for  $\text{Al}^{3+}$  in pure water," *Journal of Photochemistry and Photobiology A: Chemistry*, vol. 418, Article ID 113431, 2021.
- [2] F. Ahmed, S. Iqbal, and H. Xiong, "Multifunctional dual emissive fluorescent probe based on europium-doped carbon dots (Eu-TCA/NCDs) for highly selective detection of chloramphenicol,  $\text{Hg}^{2+}$  and  $\text{Fe}^{3+}$ ," *Environmental Science: Nano*, vol. 9, no. 8, pp. 2624–2637, 2022.
- [3] S. I. Vallejos, A. Muñoz, S. Ibeas, F. Serna, F. C. García, and J. M. García, "Forced solid-state interactions for the selective "Turn-On" fluorescence sensing of aluminum ions in water using a sensory polymer substrate," *ACS Applied Materials and Interfaces*, vol. 7, no. 1, pp. 921–928, 2015.
- [4] L.-x. Zhao, X.-l. He, K.-b. Xie et al., "A novel isophorone-based fluorescent probe for recognition of  $\text{Al}^{3+}$  and its bioimaging in cells and plants," *Spectrochimica Acta Part A: Molecular and Biomolecular Spectroscopy*, vol. 285, Article ID 121882, 2023.
- [5] J. Liu and G. Lewis, "Environmental toxicity and poor cognitive outcomes in children and adults," *Journal of Environmental Health*, vol. 76, no. 6, pp. 130–138, 2014.
- [6] J. E. Gall, R. S. Boyd, and N. Rajakaruna, "Transfer of heavy metals through terrestrial food webs: a review," *Environmental Monitoring and Assessment*, vol. 187, no. 4, p. 201, 2015.
- [7] V. N. Mehta and S. K. Kailasa, "Malonamide dithiocarbamate functionalized gold nanoparticles for colorimetric sensing of  $\text{Cu}^{2+}$  and  $\text{Hg}^{2+}$  ions," *RSC Advances*, vol. 5, no. 6, pp. 4245–4255, 2015.
- [8] N. Şatıroğlu and İ. Tokgöz, "Cloud point extraction of aluminum (III) in water samples and determination by electrothermal atomic absorption spectrometry, flame atomic absorption spectrometry and UV-visible spectrophotometry," *International Journal of Environmental Analytical Chemistry*, vol. 90, no. 7, pp. 560–572, 2010.
- [9] A. Kumar, M. Bhatt, G. Vyas, S. Bhatt, and P. Paul, "Sunlight induced preparation of functionalized gold nanoparticles as recyclable colorimetric dual sensor for aluminum and fluoride in water," *ACS Applied Materials and Interfaces*, vol. 9, no. 20, pp. 17359–17368, 2017.
- [10] Z. Qiu, J. Shu, and D. Tang, "Bioresponsive release system for visual fluorescence detection of carcinoembryonic antigen from mesoporous silica nanocontainers mediated optical color on quantum dot-enzyme-impregnated paper," *Analytical Chemistry*, vol. 89, no. 9, pp. 5152–5160, 2017.
- [11] J. Shu and D. Tang, "Current advances in quantum-dots-based photoelectrochemical immunoassays," *Chemistry--An Asian Journal*, vol. 12, no. 21, pp. 2780–2789, 2017.
- [12] Z. Gao, M. Xu, L. Hou, G. Chen, and D. Tang, "Magnetic bead-based reverse colorimetric immunoassay strategy for sensing biomolecules," *Analytical Chemistry*, vol. 85, no. 14, pp. 6945–6952, 2013.
- [13] Z. Qiu, J. Shu, and D. Tang, "Near-infrared-to-ultraviolet light-mediated photoelectrochemical aptasensing platform for cancer biomarker based on core-shell  $\text{NaYF}_4: \text{Yb}, \text{Tm} @ \text{TiO}_2$  upconversion microrods," *Analytical Chemistry*, vol. 90, no. 1, pp. 1021–1028, 2018.
- [14] W. Lai, Q. Wei, M. Xu, J. Zhuang, and D. Tang, "Enzyme-controlled dissolution of  $\text{MnO}_2$  nanoflakes with enzyme cascade amplification for colorimetric immunoassay," *Biosensors and Bioelectronics*, vol. 89, pp. 645–651, 2017.
- [15] W. Lai, Q. Wei, J. Zhuang, M. Lu, and D. Tang, "Fenton reaction-based colorimetric immunoassay for sensitive detection of brevetoxin B," *Biosensors and Bioelectronics*, vol. 80, pp. 249–256, 2016.
- [16] Y. Dong, L. Ding, X. Jin, and N. Zhu, "Silver nanoparticles capped with chalcon carboxylic acid as a probe for colorimetric determination of cadmium (II)," *Microchimica Acta*, vol. 184, no. 9, pp. 3357–3362, 2017.
- [17] B. A. García Grajeda, S. G. Soto Acosta, S. A. Aguila et al., "Selective and colorimetric detection of  $\text{Ba}^{2+}$  ions in aqueous solutions using 11-mercaptopundecylphosphonic acid functionalized gold nanoparticles," *RSC Advances*, vol. 7, no. 50, pp. 31611–31618, 2017.
- [18] V. N. Mehta, J. V. Rohit, and S. K. Kailasa, "Functionalization of silver nanoparticles with 5-sulfoanthranilic acid dithiocarbamate for selective colorimetric detection of  $\text{Mn}^{2+}$  and  $\text{Cd}^{2+}$  ions," *New Journal of Chemistry*, vol. 40, no. 5, pp. 4566–4574, 2016.

- [19] P. Joshi, M. Nair, and D. Kumar, "pH-controlled sensitive and selective detection of Cr (III) and Mn (II) by using clove (*S. aromaticum*) reduced and stabilized silver nanospheres," *Analytical Methods*, vol. 8, no. 6, pp. 1359–1366, 2016.
- [20] L. S. Walekar, A. H. Gore, P. V. Anbhule, V. Sudarsan, S. R. Patil, and G. B. Kolekar, "A novel colorimetric probe for highly selective recognition of  $\text{Hg}^{2+}$  ions in aqueous media based on inducing the aggregation of CPB-capped AgNPs: accelerating direct detection for environmental analysis," *Analytical Methods*, vol. 5, no. 20, pp. 5501–5507, 2013.
- [21] D. Nanda Kumar, A. Rajeshwari, S. A. Alex, N. Chandrasekaran, and A. Mukherjee, "Acetylcholinesterase inhibition-based colorimetric determination of  $\text{Hg}^{2+}$  using unmodified silver nanoparticles," *New Journal of Chemistry*, vol. 39, no. 2, pp. 1172–1178, 2015.
- [22] M. Zavalishin, G. Gamov, G. Nikitin et al., "A simple vitamin B6-based fluorescent chemosensor for selective and sensitive  $\text{Al}^{3+}$  recognition in water: a spectral and DFT study," *Microchemical Journal*, vol. 197, Article ID 109791, 2024.
- [23] P. Pratim Sarma, K. Barman, and P. K. Baruah, "Green synthesis of silver nanoparticles using *Murraya koenigii* leaf extract with efficient catalytic, antimicrobial, and sensing properties towards heavy metal ions," *Inorganic Chemistry Communications*, vol. 152, Article ID 110676, 2023.
- [24] C. Luo, Y. Wang, X. Li et al., "An optical sensor with polyaniline-gold hybrid nanostructures for monitoring pH in saliva," *Nanomaterials*, vol. 7, no. 3, p. 67, 2017.
- [25] M. Sharifi-Rad, H. S. Elshafie, and P. Pohl, "Green synthesis of silver nanoparticles (AgNPs) by *Lallemantia royleana* leaf Extract: their Bio-Pharmaceutical and catalytic properties," *Journal of Photochemistry and Photobiology A: Chemistry*, vol. 448, Article ID 115318, 2024.
- [26] B. Kumar, K. Smita, and L. Cumbal, "Biosynthesis of silver nanoparticles using lavender leaf and their applications for catalytic, sensing, and antioxidant activities," *Nanotechnology Reviews*, vol. 5, no. 6, pp. 521–528, 2016.
- [27] K. C. Noh, Y. S. Nam, H. J. Lee, and K. B. Lee, "A colorimetric probe to determine  $\text{Pb}^{2+}$  using functionalized silver nanoparticles," *The Analyst*, vol. 140, no. 24, pp. 8209–8216, 2015.
- [28] V. Tharmaraj and J. Yang, "Sensitive and selective colorimetric detection of  $\text{Cu}^{2+}$  in aqueous medium via aggregation of thiomalic acid functionalized Ag nanoparticles," *The Analyst*, vol. 139, no. 23, pp. 6304–6309, 2014.
- [29] W. Ha, J. Yu, R. Wang, J. Chen, and Y. Shi, "Green colorimetric assay for the selective detection of trivalent chromium based on *Xanthoceras sorbifolia* tannin attached to gold nanoparticles," *Analytical Methods*, vol. 6, no. 15, pp. 5720–5726, 2014.
- [30] K. M. Tripathi, T. S. Tran, Y. J. Kim, and T. Kim, "Green fluorescent onion-like carbon nanoparticles from flaxseed oil for visible light induced photocatalytic applications and label-free detection of Al (III) ions," *ACS Sustainable Chemistry and Engineering*, vol. 5, no. 5, pp. 3982–3992, 2017.
- [31] X. Li, J. Wang, L. Sun, and Z. Wang, "Gold nanoparticle-based colorimetric assay for selective detection of aluminium cation on living cellular surfaces," *Chemical Communications*, vol. 46, no. 6, pp. 988–990, 2010.
- [32] S. Bothra, R. Kumar, and S. K. Sahoo, "Pyridoxal derivative functionalized gold nanoparticles for colorimetric determination of zinc (II) and aluminium (III)," *RSC Advances*, vol. 5, no. 118, pp. 97690–97695, 2015.
- [33] P. Huang, J. Li, X. Liu, and F. Wu, "Colorimetric determination of aluminum (III) based on the aggregation of Schiff base-functionalized gold nanoparticles," *Microchimica Acta*, vol. 183, no. 2, pp. 863–869, 2016.
- [34] S. Sooksin, V. Promarak, S. Ittisanronnachai, and W. Ngeontae, "A highly selective fluorescent enhancement sensor for  $\text{Al}^{3+}$  based nitrogen-doped carbon dots catalyzed by  $\text{Fe}^{3+}$ ," *Sensors and Actuators B: Chemical*, vol. 262, pp. 720–732, 2018.
- [35] R. Painuli, P. Joshi, and D. Kumar, "Aluminon functionalized silver nanoparticles for the colorimetric detection of aqueous Al (III)," *Materials Chemistry and Physics*, vol. 239, Article ID 122318, 2020.
- [36] P. Ruíz del Portal-Vázquez, G. López-Pérez, R. Prado-Gotor, C. Román-Hidalgo, and M. J. Martín-Valero, "Citrate and polyvinylpyrrolidone stabilized silver nanoparticles as selective colorimetric sensor for aluminum (III) ions in real water samples," *Materials*, vol. 13, no. 6, p. 1373, 2020.
- [37] M. Ateeq, M. R. Shah, N. Ain et al., "Green synthesis and molecular recognition ability of patuletin coated gold nanoparticles," *Biosensors and Bioelectronics*, vol. 63, pp. 499–505, 2015.